Inorg. Chem. **2006**, *45*, 4938–4950

Chemistry of 2,2,6,6,-Tetramethyl-3,5-heptanedione (Hthd) Modification of Zirconium and Hafnium Propoxide Precursors

Gerald I. Spijksma,[†] Henny J. M. Bouwmeester, and Dave H. A. Blank

Inorganic Materials Science, Faculty of Science & Technology, and Mesa$^+$ Institute for Nanotechnology, University of Twente, P.O. Box 217, 7500 AE, Enschede, The Netherlands

Andreas Fischer

Inorganic Chemistry, Royal University of Technology, 100 44, Stockholm, Sweden

Marc Henry

Université Louis Pasteur, Laboratoire de Chimie Moléculaire et de RMN du Solide, Institut Le Bel, 4 Rue Blaise Pascal, 67070 Strasbourg, France

Vadim G. Kessler*

Department of Chemistry, SLU, Box 7015, 75007 Uppsala, Sweden

Received September 29, 2005

The modification of different zirconium propoxide and hafnium propoxide precursors with 2,2,6,6,-tetramethyl-3,5-heptanedione (Hthd) was investigated by characterization of the isolated modified species. The complexes $[Zr(O^nPr)_3(thd)]_2$, $[Zr(O^nPr)(O^iPr)_2(thd)]_2$, $Zr(O^iPr)(thd)_3$, $[Hf(O^nPr)_3(thd)]_2$, and $Hf(O^iPr)(thd)_3$ were isolated and characterized. The structure of the *n*-propoxide analogue of $Zr(O^iPr)(thd)_3$ could not be refined, but its existence was clearly demonstrated by XRD and ^{1}H NMR. The modification of the propoxide precursors involves mono- and trisubstituted intermediate compounds and does not involve a disubstituted compound; thus, the commercial product that is claimed to be "$Zr(O^iPr)_2(thd)_2$" and is most commonly used for the MOCVD preparation of ZrO_2 does not exist. No evidence was found for the presence of such a compound in either zirconium- or hafnium-based systems. Formation of the dimeric hydroxo-di-thd-substituted complex, $[Hf(OH)(O^iPr)(thd)_2]_2$, which could be isolated only for hafnium-based systems, occurs on microhydrolysis. All heteroleptic intermediates are eventually transformed to the thermodynamically stable $Zr(thd)_4$ or $Hf(thd)_4$. The compounds obtained from isopropoxide precursors showed a higher stability than those with *n*-propoxide ligands or a combination of both types. In addition, it is important to note that residual alcohol facilitates the transformation and strongly enhances its rate. The unusually low solubility and volatility of $M^{IV}(thd)_4$ has been shown to be due to close packing and strong van der Waals interactions in the crystal structures of these compounds.

Introduction

Zirconia is an important material that is widely used in structural ceramics,[1,2] gas sensors,[3−4] catalysts,[6−8] and dense dielectric and ferroelectric films in electronics.[9,10] It is an attractive candidate for very large scale integrated circuits and as a gate dielectric in metal-oxide semiconductor (MOS)

* To whom correspondence should be addressed. Tel: 46 18 671541. Fax: 46 18 673476. E-mail: Vadim.Kessler@kemi.slu.se.

[†] Also connected to Department of Chemistry, SLU, Box 7015, 75007 Uppsala, Sweden.

(1) Vacassy, R. J.; Guizard, C.; Palmeri, J.; Cot, L. *Nanostruct. Mater.* **1998**, *10*, 77.
(2) Xia, C. R.; Cao, H. Q.; Wang, H.; Yang, P. H.; Meng, G. Y.; Peng, D. K. *J. Membr. Sci.* **1999**, *162*, 181.
(3) Kurosawa, H.; Yan, Y.; Miura, N.; Yamazoe, N. *Solid State Ionics* **1999**, *79*, 338.
(4) Rodrigues, C. M. S.; Labrincha, J. A.; Marques, F. M. B. *Solid State Ionics* **2000**, *136−137*, 671.
(5) Miura, M.; Nakatou, S.; Zhuiykov, N. *Sens. Actuators, B* **2003,** *93*, 221.
(6) Li, Y. W.; He, D. H.; Cheng, Z. X.; Su, C. L.; Li, J. R.; Zhu, Q. M. *J. Mol. Catal. A: Chem.* **2001**, *175*, 267.
(7) Haruta, M.; Kobayashi, T.; Sano, H.; Yamada, N. *Chem. Lett.* **1987,** *829*, 405.
(8) Knell, A.; Barnickel, P.; Baiker, A.; Wokaun, A. *J. Catal.* **1992,** *137*, 306.

10.1021/ic051674j CCC: $33.50
Published on Web 06/03/2006

devices because of its high dielectric constant (~25).[11] In addition, zirconia also has a beneficially high band gap (5.8−7.8 eV)[11] and thermal compatibility with contemporary CMOS processes.[12] Increasing interest in the miniaturization of devices and the development of nanotechnology applications urges improvement of techniques for the controlled preparation of zirconium-oxide-based materials.

Chemical vapor deposition is compatible with semiconductor processing, which makes it attractive for the preparation of microelectronics. The advantages of this process include the control of composition and the ability to scale it up to large amounts.[12] If metal−organic precursors are used, as in the present study, the deposition technique is referred to as MOCVD (metal−organic vapor deposition). The selection of a precursor is a fundamental aspect of the MOCVD process. The chemical compatibility of the precursor in solution and in the vapor phase is necessary for maximum efficiency.[12] In addition, solution stability and thermal stability during vapor-phase transport are extremely critical for process reproducibility. It may be considered obvious that the precursor composition should not change during storage after its preparation and before it is used, i.e., the precursor should be shelf stable.

Zirconium atoms in the molecules of homoleptic alkoxide complexes have unsaturated coordination, which makes the precursors extremely sensitive to hydrolysis and pyrolysis. Another drawback of unmodified precursors (e.g., zirconium isopropoxide) is their relatively low volatility, which requires high deposition and substrate temperatures and leads to carbon contamination.

A general method for moderating reactivity and improving the volatility is by the exchange of alkoxide ligands for chelating organic ligands.[12−14] The first generation CVD precursors of oxides were zirconium and hafnium alkoxides modified by β-diketones.[13] Modification with 2,2,6,6,-tetramethyl-3,5-heptanedione (Hthd) provides higher volatility by the improved shielding effect on the metal atom by the larger terminal organic groups.

The replacement of part of the alkoxide ligands of zirconium and hafnium isoproxide precursors has been reported. Introduction of 1 thd ligand per zirconium or hafnium atom provided dimeric $[M(O^iPr)_3(thd)]_2$.[15] The behavior of these precursors in solution is not understood,[15] and there is only a limited knowledge dealing with the preparation of films by MOCVD[16−18] starting from this precursor.

A significantly more often applied MOCVD precursor is "$Zr(O^iPr)_2(thd)_2$".[19−25] This nowadays commercially available product was initially claimed to be a single compound.[17] However, in later publications, it was said to be a stoichiometric mixture of mono- and dimeric structures and even suspected to be prone to some decomposition reactions.[15,23] Thus, despite it being commercially available, this product had not been fully characterized and even its existence had not been proved unequivocally.

The complete replacement of alkoxide ligands by Hthd leads to the formation of the complex $Zr(thd)_4$ Several studies have been devoted to the synthesis of this compound,[26] however, no structure determination for it has been published. The behavior of the compound in solution and gas phase is remarkable. The compound is, despite very good shielding of the metal atom by the bulky organic ligands, relatively poorly soluble in hydrocarbon solvents and by far not as volatile as one would expect. Nevertheless, it is frequently applied as a precursor in MOCVD applications.[21,24,25,27−29]

It can be concluded that the chemistry involved in the modification of zirconium and hafnium isopropoxide precursors by Hthd is not clear. The understanding of this chemistry can be of great importance for the development of future-generation CVD oxide precursors and for the preparation of materials from the precursors modified by Hthd. The search for an understanding of the principles in solution stability and volatility of alkoxide-β-diketonate complexes was the main driving force in the present study.

We have thus carried out modification of zirconium and hafnium propoxide precursors, including zirconium *n*-propoxide, a mixed ligand precursor,[30,31] $[Zr(O^nPr)(O^iPr)_3(^iPrOH)]_2$, and hafnium *n*- and isopropoxide, and report here the isolation and structural characterization of the products

(9) Hoffman, S.; Klee, M.; Waser, R. *Integr. Ferroelectr.* **1995**, *10*, 155.
(10) Klee, M.; Mackens, U.; Hermann, W.; Bathelt, E. *Integr. Ferroelectr.* **1995**, *11*, 247.
(11) Wilk, G. D.; Wallace, R. M.; Anthony, J. M. *J. Appl. Phys.* **2001**, *89*, 5243.
(12) Jones, A. C.; Aspinall, H. C.; Chalker, P. R.; Potter, R. J.; Kukli, K.; Rahtu, A.; Ritala, M.; Leskelä, M. *J. Mater. Chem.* **2004**, *14*, 3101.
(13) Hubert-Pfalzgraf, L. G. *J. Mater. Chem.* **2004**, *14*, 3113.
(14) Leedham, T. J.; Jones, A. C.; Wright, P. J.; Crosbie, M. J.; Williams, D. J.; Davies, H. O.; O'Brien, P. *Integr. Ferroelectr.* **1999**, *26*, 767.
(15) Fleeting, K. A.; O'Brien, P.; Otway, D. J.; White, A. J. P.; Williams, D. J.; Jones, A. C. *Inorg. Chem.* **1999**, *38*, 1432.
(16) Jones, A. C.; Leedham, T. J.; Wright, P. J.; Williams, D. J.; Crosbie, M. J.; Davies, H. O.; Fleeting, K. A.; O'Brien, P. *J. Eur. Ceram. Soc.* **1999**, *19*, 1431.
(17) Jones, A. C.; Leedham, T. J.; Wright, P. J.; Crosbie, M. J.; Lane, P. A.; Williams, D. J.; Fleeting, K. A.; Otway, D. J.; O'Brien, P. *Chem. Vap. Deposition* **1998**, *4*, 46.
(18) Kim, D. H.; Na, J. S.; Rhee, S. W. *J. Electrochem. Soc.* **2001**, *148*, C668.
(19) Chen, H.-W.; Huang, T.-Y.; Landheer, D.; Wu, X.; Moisa, S.; Sproule, G. I.; Chao, T.-S. *J. Electrochem. Soc.* **2002**, *149*, F49.
(20) Chen, H.-W.; Landheer, D.; Wu, X.; Moisa, S.; Sproule, G. I.; Chao, T.-S.; Huang, T. Y. *J. Vac. Sci. Technol., A* **2002**, *20*, 1145.
(21) Ahn, H.; Chen, H.-W.; Landheer, D.; Wu, X.; Chou, L. J.; Chao, T.-S. *Thin Solid Films* **2004**, *455−456*, 318.
(22) Chen, H.-W.; Huang, T.-Y.; Landheer, D.; Wu, X.; Moisa, S.; Sproule, G. I.; Kim, J. K.; Lennard, W. N.; Chao, T.-S. *J. Electrochem. Soc.* **2003**, *150*, C465.
(23) Jones, A. C.; Leedham, T. J.; Wright, P. J.; Crosbie, M. J.; Williams, D. J.; Fleeting, K. A.; Davies, H. O.; Otway, D. J.; O'Brien, P. *Chem. Vap. Deposition* **1998,** *4*, 197.
(24) Roeder, J. F.; Baum, T. H.; Bilodeau, S. M.; Stauf, G. T.; Ragaglia, C.; Russell, M. W.; Van Buskirk, P. C. *Adv. Mater. Opt. Electron.* **2000**, *10*, 145.
(25) Chen, I.-S.; Hendrix, B. C.; Bilobeau, S. M.; Wang, Z.; Xu, C.; Johnston, S.; Van Buskirk, P. C.; Baum, T. H.; Roeder, J. F. *Jpn. J. Appl. Phys.* **2002**, *41*, 6695.
(26) Si, J.; Desu, S. B.; Tsai, C. Y. *J. Mater. Res.* **1994**, *9*, 1721
(27) Dubourdieu, C.; Kang, S. B.; Li, Y. Q.; Kulesha, G.; Gallois, B. *Thin Solid Films* **1999**, *339*, 165.
(28) Chevalier, S.; Kilo, M.; Borchardt, G.; Larpin, J. P. *Appl. Surf. Sci.* **2003**, *205*, 188.
(29) Putkonen, M.; Niinistö, L. *J. Mater. Chem.* **2001**, *11*, 3141.
(30) Seisenbaeva, G. A.; Gohil, S.; Kessler, V. G. *J. Mater. Chem.* **2004**, *14*, 3177.
(31) Spijksma, G. I. P.hD. thesis, University of Twente, Twente, The Netherlands, 2006.

of these reactions. Special attention was paid to the investigation of their solution and solid-state stability in time by NMR and by monitoring their evaporation behavior by mass spectrometry.

Experimental Section

All manipulations were carried out in a dry nitrogen atmosphere using the Schlenk technique or a glovebox. Hexane and toluene (Merck) were dried by distillation after refluxing with $LiAlH_4$. 2,2,6,6,-Tetramethyl-3,5-heptanedionate (Hthd) was purchased from Aldrich and used without further purification. The commercially available "$Zr(thd)_2(O^iPr)_2$" was purchased from Aldrich.

IR spectra were registered with a Jasco-40 FT-IR spectrometer in the interval 4000−700 cm^{-1} for compounds **1**−**4** and **7** and **8** and with a Bruker Tensor-27 FT-IR spectrometer in the interval 1000−400 cm^{-1} for the same compounds. IR spectra of compounds **5** and **6** were recorded with a Perkin−Elmer Spectrum 100 FT-IR spectrometer in the interval 4000−400 cm^{-1}. ^1H NMR spectra were recorded in $CDCl_3$ for all compounds on a Bruker 400 MHz spectrometer at 243 K. The results of microanalysis (C, N, H) were obtained by the chemical analysis group of the University of Twente, The Netherlands, and at MikroKemi AB in Uppsala using the combustion technique.

Synthesis. The zirconium propoxide precursors used in this work as starting materials are zirconium isopropoxide ($[Zr(O^iPr)_4(^iPrOH)]_2$ 99.9%), 70 wt % solution of $Zr(O^nPr)_4$ (both purchased from Aldrich), and $[Zr(O^nPr)(O^iPr)_3(^iPrOH)]_2$ which was prepared according to a recently developed technique.[30,31] The zirconium isoproxide was dissolved and recrystallized from toluene prior to use in order to remove impurities. The hafnium isopropoxide was prepared by anodic oxidation of hafnium metal in 2-propanol[32] and recrystallized from toluene. Hafnium *n*-propoxide was prepared by anodic oxidation of hafnium metal in *n*-propanol.[31] All the different precursors were modified with various equivalent amounts of Hthd according to the techniques described below. The exact composition of single crystals **1**−**8** was established with single-crystal X-ray studies.

$[Zr(O^nPr)_3(thd)]_2$ (1). Commercial 70% zirconium *n*-propoxide in *n*-propanol was dried (weight, 0.754 g (1.95 mmol)) under a vacuum (0.1 mmHg) and redissolved in 2 mL of hexane. After addition of 0.36 g (1.95 mmol) of Hthd, the yellowish sample was placed overnight in the freezer at −30 °C. The next day, a significant amount of product had been formed; the solution was decanted, and the obtained colorless crystals were identified as **1** (yield: 0.60 g, 54%). Calcd for $Zr_2C_{40}H_{80}O_{10}$: C, 55.13; H, 8.94. Found: C, 54.73; H, 8.7. IR (cm^{-1}): 1575 s, 1538 m, 1506 s, 1469 sh, 1359 m, 1294 m, 1247 w, 1226 m, 1176 w, 1147 s, 1079 w, 1026 w, 995 w, 1079 m, 871 s, 794 sh, 761 br, 614 s, 582 m, 554 m, 494 sh, 481 s, 420 s br. ^1H NMR ($CDCl_3$, 400 MHz, 243 K): δ 0.74 (6H, triplet, Me_{OnPr}, J_{H-H} = 6.0 Hz), 0.80 (12H, triplet, Me_{OnPr}, J_{H-H} = 6.0 Hz), 1.17 (36H, singlet, Me_{thd}), 1.41 (12H, overlapping, CH_{2OnPr}), 3.81 (8H, unresolved, terminal CH_{OnPr}), 3.93 (4H, unresolved, bridging CH_{OnPr}), 5.87 (2H, singlet, CH_{thd}).

$[Zr(O^nPr)(O^iPr)_2(thd)]_2$ (2). The prepared $[Zr(O^nPr)(O^iPr)_3(^iPrOH)]_2$ (1.84 g, 4.76 mmol) was dissolved in 2 mL of hexane, and 0.88 g (4.77 mmol) Hthd was added. The sample was placed at −30 °C overnight for crystallization. The obtained crystals turned out to be too small for XRD analysis. After the addition of 2 mL of hexane, the clear solution was again placed for crystallization. The solution was decanted, and the obtained crystals (yield: 1.62 g, 60%) were identified as **2**. Calcd for $Zr_2C_{40}H_{80}O_{10}$: C, 55.13; H, 8.94. Found: C, 55.21; H, 8.8. IR (cm^{-1}): 1589 sh, 1579 s, 1559 w, 1539 w, 1507 s, 1293 w, 1241 w, 1227 w, 1149 s, 1020 m, 966 w, 872 s, 800 sh, 765 sh, 613 s, 584 m, 548 m, 480 s, 420 sh. ^1H NMR ($CDCl_3$, 400 MHz, 243 K): δ 0.73 (3H, unresolved, CH_{3OnPr}), 1.04 (6H, unresolved, Me_{OiPr}), 1.14 (18H, singlet, Me_{thd}), 1.44 (2H, unresolved, CH_{2OnPr}), 3.87 (2H, unresolved, CH_{2OnPr}), 4.24 (2H, unresolved, CH_{OiPr}), 5.83 (1H, singlet, CH_{thd}).

$[Zr(O^iPr)(thd)_3]$ (3). Compound **3** was obtained from two different syntheses. (a) To a solution of $[Zr(O^nPr)(O^iPr)_3(^iPrOH)]_2$ (1.32 g, 3.41 mmol) in 2 mL of hexane was added 1.25 g (6.78 mmol) of Hthd (i.e., 2 mol equiv). The solution was stored overnight at −30 °C and subsequently dried under a vacuum (0.1 mmHg). The resulting white solid was redissolved in 1.5 mL of hexane and again stored at −30 °C for crystallization. The next day, the solution was decanted, and the obtained colorless crystals (yield: 1.0 g, 39%) were identified as **3**. IR and element analysis were performed.

(b) The analogous modification with 2 mol equiv of Hthd was performed, using zirconium isopropoxide as precursor instead. The zirconium isopropoxide (0.59 g, 1.53 mmol) was dissolved in 3 mL of a mixture of hexane and toluene (volume ratio 2:1), and 0.58 g (3.15 mmol) of Hthd was added. The solution was placed at −30 °C overnight; the solvents were subsequently decanted from the obtained crystals. The crystals (yield: 0.27 g, 23%) were identified, on the basis of their unit cell parameters obtained by XRD, as $[Zr(O^iPr)_3(thd)]_2$.[15] The decanted solution was dried under a vacuum (0.1 mmHg), and the obtained white solids were redissolved in 2 mL of hexane. After being stored overnight at −30 °C, crystals that were again identified as $[Zr(O^iPr)_3(thd)]_2$ were obtained. The solution that was decanted from the crystals was stored on the lab bench in a flask with a serum cap stopper. After ∼4 weeks, the hexane had diffused through the stopper, and big platelet crystals, identified as **3**, had formed in the flask. Yield: 0.36 g (about 40%). Calcd for $ZrC_{36}H_{64}O_7$: C, 61.80; H, 9.15. Found: C, 61.41; H, 9.0. IR (cm^{-1}): 2726 w, 1573 w, 1537 w, 1506 s, 1403 w, 1359 m, 1294 m, 1247 sh, 1226 s, 1172 w, 1147 s, 1080 w, 1022 m, 968 m, 935 w, 873 s, 847 w, 794 s, 761 w, 738 m, 614 vs, 582 m, 494 s, 481 m, 421 m. ^1H NMR ($CDCl_3$, 400 MHz, 243 K): δ 1.02 (6H, doublet, Me_{OiPr}), 1.07 (54H, unresolved, Me_{thd}), 4.36 (1H, septet, CH_{OiPr}, J_{H-H} = 6.0 Hz), 5.80 (3H, singlet, CH_{thd}).

We also attempted to prepare a trisubstituted compound from zirconium *n*-propoxide. Commercial 70 wt % zirconium *n*-propoxide in *n*-propanol was dried (weight: 0.61 g (1.58 mmol)) under a vacuum (0.1 mmHg) and redissolved in 2 mL of hexane. After the addition of 0.86 g (4.67 mmol) of Hthd, the yellowish sample was dried under a vacuum (0.1 mmHg), and the remaining product was dissolved in 1 mL hexane. The sample was stored on the lab bench in a flask with a serum cap. After ∼4 weeks, the hexane had diffused through the stopper, and two types of crystals had formed in the flask. One of the crystal types was not of X-ray quality; the obtained NMR spectra on this compound indicated that it was the product aimed for trisubstituted zirconium *n*-propoxide. ^1H NMR ($CDCl_3$, 400 MHz, 243 K): δ 0.72 (3H, triplet, Me_{OnPr}), 1.17 (54H, unresolved, Me_{thd}), 1.38 (2H, sextet, CH_{2OnPr}), 4.05 (2H, triplet, CH_{2OnPr}), 5.80 (3H, singlet, CH_{thd}). The other crystal type, which was of X-ray quality, was identified as **7a**.

$[Hf(O^nPr)_3(thd)]_2$ (4). Hafnium *n*-propoxide (1.11 g, 2.34 mmol) was dissolved in 2 mL of hexane. After the addition of 0.43 g (2.34 mmol) of Hthd, the yellowish sample was dried under a vacuum (0.1 mmHg); the residual product was dissolved in 1 mL of hexane. The sample was stored on the lab bench in a flask with a serum

(32) Turevskaya, E. P.; Kozlova, N. I.; Turova, N. Y.; Belokon, A. I.; Berdyev, D. V.; Kessler, V. G.; Grishin, Y. K. *Russ Chem. Bull.* **1995**, *44*, 734.

cap. After ~4 weeks, the hexane had diffused through the stopper, and single crystals had formed in the flask. The obtained crystals were identified as **4**. Calcd for $Hf_2C_{40}H_{80}O_{10}$: C, 44.56; H, 7.48. Found: C, 43.64; H, 7.21. IR (cm^{-1}): 1575 s, 1559 m, 1538 m, 1507 s, 1469 sh, 1376 s, 1151 s, 871 s, 622 m, 585 s, 544 s, 479 s, 459 s, 405 s br. ^1H NMR ($CDCl_3$, 400 MHz, 243 K): δ 0.74 (6H, triplet, Me_{OnPr}), 0.80 (12H, triplet, Me_{OnPr}), 1.17 (36H, singlet, Me_{thd}), 1.41 (12H, overlapping, CH_{2OnPr}), 3.81 (8H, unresolved, terminal CH_{2OnPr}), 3.93 (4H, unresolved, bridging CH_{2OnPr}), 5.87 (2H, singlet, CH_{thd}).

Isolation of $[Hf(O^iPr)(thd)_3]$ (5) and $[Hf(O^iPr)(OH)(thd)_2]_2$ (6). Hafnium isopropoxide (weight: 0.85 g, 1.79 mmol) was dissolved in 6 mL of a mixture of hexane and toluene (volume ratio 1:2). After the addition of 0.80 g (4.34 mmol) of Hthd, i.e., 2.5 mol equiv, the solvent was removed from the mixture under a vacuum (0.1 mmHg). The obtained solid product was subsequently redissolved in 2 mL of hexane. The obtained solution was left to crystallize at room temperature by diffusion of the solvent through the serum cap. After ~1 week, some crystals had formed. The remaining solution was decanted from the obtained crystals and transferred to another flask that was left at room temperature for further crystallization. The obtained crystals were identified as $[Hf(O^iPr)_3(thd)]_2$.[15] After ~2 weeks, a new product was obtained and turned out to consist of a mixture of crystals. Both types of crystals were of X-ray quality; they were identified as **5** and $[Hf(O^iPr)(OH)(thd)_2]_2$ (**6**).

$[Hf(O^iPr)(thd)_3]$ (5) Synthesis. (Warning: the process can be carried out successfully only if freshly distilled solvents are applied.) Hafnium isopropoxide (weight: 0.92 g, 1.94 mmol) was dissolved in 5 mL of toluene. After the addition of 2.3 equiv of Hthd (0.82 g, 4.46 mmol), the solution was evaporated to dryness in a vacuum (0.1 mmHg). The obtained solid product was subsequently redissolved in 2 mL of hexane and left for crystallization overnight at −30 °C. The solution was removed from the crystalline product identified as $[Hf(O^iPr)_3(thd)]_2$[15] (0.48 g, 0.89 mmol, ~ 46% yield) by syringe and transferred to a different flask, where it was warmed to room temperature and reduced in a vacuum to approximately 2/3 of the initial volume (until the start of crystallization). The evacuation was aborted, and the slightly viscous solution was again removed from the small crop of crystals formed and evaporated to dryness. The crystalline residue (transparent, almost rectangular shaped plates) was identified as $[Hf(O^iPr)(thd)_3]$ (**5**). Yield: 0.64 g (42%). Calcd for $C_{36}H_{64}O_7Hf$: C, 54.92; H, 8.19. Found: C, 54.68; H, 8.0. IR (cm^{-1}): 1574 m, 1536 m, 1505 s, 1403 m, 1359 m, 1294 m, 1247 sh, 1226 s, 1176 w, 1147 s, 1079 w, 1022 m, 968 m, 935 w, 871 m, 847 w, 794 s, 761 w, 738 m, 614 m, 580 m, 460 m. ^1H NMR ($CDCl_3$, 400 MHz, 243 K): δ 1.02 (6H, doublet, Me_{OiPr}), 1.07 (54H, unresolved, Me_{thd}), 4.36 (1H, septet, CH_{OiPr}), 5.80 (3H, singlet, CH_{thd}).

$[Hf(O^iPr)(OH)(thd)_2]_2$ (6) Synthesis. Hafnium isopropoxide (weight: 1.13 g, 2.38 mmol) was dissolved in 4.5 mL of toluene. A clear solution made by mixing 0.88 g of Hthd, 0.04 g of water, and 3 mL of 2-propanol was quickly added to the alkoxide solution with vigorous stirring. The clear solution obtained was evaporated to dryness in a vacuum, leaving a crude product. The latter was redissolved in 1.5 mL of hexane on reflux and left for crystallization in a freezer at −30 °C overnight. The precipitated needle-shaped crystals were separated by decantation and dried in a vacuum. Yield: 1.30 g (88%). Calcd for $C_{50}H_{92}O_{12}Hf_2$: C, 48.34; H, 7.47. Found: C, 47.96; H, 7.3. IR (cm^{-1}): 3690 m s, 3440 w, 3356 w br, 3178 w br, 1591 m, 1574 s, 1551w, 1535 m, 1505 s, 1404 s, 1358 m, 1293 m, 1246 m, 1226 m, 1174 s, 1147 s, 1076 w, 1055 w, 1021 m, 967 m, 930 w, 909 vw, 807 w, 793 m, 759 w, 737 w, 614 s, 482 s, 418 w. ^1H NMR ($CDCl_3$, 400 MHz, 273 K), δ: 1.09 (27H, singlet, Me_{thd}), 1.14 (9H, singlet, Me_{thd}), 1.23 (6H, doublet, Me_{OiPr}, J_{H-H} = 10.6 Hz), 4.45 (1H, septet, J_{H-H} = 6.05 Hz), 5.67 (2H, singlet, CH_{thd}).

$Zr(thd)_4$ (7a and 7b). Commercial 70 wt % zirconium *n*-propoxide in *n*-propanol was dried (weight: 1.59 g (4.10 mmol)) under a vacuum (0.1 mmHg) and redissolved in 1 mL of hexane. A white solid formed instantly upon the addition of 3.0 g (16.3 mmol) of Hthd. Additional hexane was added (2.5 mL); the mixture was refluxed for 30 min, resulting in a clear yellowish solution. The solution was placed in the freezer at −30 °C for crystallization, and an almost-quantitative yield of the product was obtained. However, no X-ray quality crystals could be isolated. The obtained product was dried and redissolved upon heating in 14 mL of 2-propanol. The solution was left to crystallize at room temperature and produced X-ray quality crystals. The initially crystallized batch of platelets was characterized as **7a**, whereas the needles formed later from the diluted solution turned to possess the structure **7b**. Calcd for $ZrC_{44}H_{76}O_8$: C, 63.98; H, 9.37. Found: C, 64.14; H, 9.42. IR (cm^{-1}): 2854 s, 1593 sh, 1574 s, 1545 w, 1534 m, 1504 m, 1403 w, 1298 w, 1250 w, 1226 m, 1179 sh, 1148 m, 1620 w, 967 w, 935 w, 873 s, 792 m, 760 sh, 722 s, 613 s, 492 m, 481 m, 420 sh. ^1H NMR ($CDCl_3$, 400 MHz, 243 K): δ 1.05 (72H, singlet, Me_{thd}), 5.62 (4H, singlet, CH_{thd}).

$Hf(thd)_4$ (8). Hafnium isopropoxide (weight: 1.03 g (2.17 mmol)) was dissolved in a 9 mL mixture of hexane and toluene (volume ratio 1:2). After the addition of 1.61 g (8.74 mmol) of Hthd, the mixture was refluxed for 30 min. Subsequently, the solvent was removed from the solution under a vacuum (0.1 mmHg). The obtained solid product was redissolved upon heating in 30 mL of 2-propanol. The solution was left for crystallization at room temperature, and X-ray quality crystals were obtained. Their structure was determined to be **8**. Calcd for $HfC_{44}H_{76}O_8$: C, 60.09; H, 8.29. Found: C, 59.26; H, 8.4. The lower values observed for C and H are possible because of the formation of hydrolyzed species during the synthesis. IR (cm^{-1}):1593 m, 1568 s, 1534 s, 1297 w, 1247 w, 1227 w, 1172 sh, 1152 m, 1077 w, 1031 w, 971 w, 866 m, 790 w, 723 s, 614 m, 543 w, 490 m, 479 s, 419 sh. ^1H NMR ($CDCl_3$, 400 MHz, 243 K): δ 1.05 (72H, singlet, Me_{thd}), 5.62 (4H, singlet, CH_{thd}).

Crystallography. Data collection for single crystals of all compounds except **7b** was carried out at 22 °C on a SMART CCD 1k diffractometer with graphite-monochromated Mo Kα radiation. All structures were solved by standard direct methods. The coordinates of the metal atoms as well as the majority of other non-hydrogen atoms were obtained from the initial solutions and for all other non-hydrogen atoms were found in subsequent difference Fourier syntheses. The structural parameters were refined by least squares using first isotropic and then, where possible (for example, not for carbon atoms in case of thd ligands disordered between several positions such as in **6**, **7a**, **7b**, and **8**, where molecules with different conformations and different orientations are sharing the same site, i.e., have the same metal-atom position, but different positions for other atoms, in the crystal structures) anisotropic approximations. The coordinates of the hydrogen atoms were calculated geometrically where possible and were included in the final refinement in the isotropic approximation for all compounds except **6**, **7a**, **7b**, and **8**, where their location is completely impossible. Full refinement of the structure of $Zr(O^nPr)(thd)_3$ was not accomplished because of rather complex unresolved disorder in the *n*-propyl radical. A general feature hindering proper refinement of these structures is the rotational disorder in the ^{t}Bu fragments of the thd ligands. In the structures of compounds **3** and

Table 1. Crystal Data and the Diffraction Experiments Details for Compounds **1**−**8**

	1	**2**	**3**	**4**	**5**
chemical composition	$C_{40}H_{80}O_{10}Zr_2$	$C_{40}H_{80}O_{10}Zr_2$	$C_{36}H_{64}O_7Zr$	$C_{40}H_{80}O_{10}Hf_2$	$C_{36}H_{64}O_7Hf$
fw	903.48	903.48	700.09	1078.02	787.36
cryst syst	triclinic	monoclinic	monoclinic	triclinic	monoclinic
space group	$P\bar{1}$	$P2(1)/c$	$P2(1)/c$	$P\bar{1}$	$P2(1)/c$
μ (mm^{-1})	0.469	0.467	0.317	4.094	2.646
a (Å)	9.407(4)	20.191(16)	10.153(3)	10.338(4)	10.27(3)
b (Å)	10.086(5)	9.753(8)	20.995(5)	21.184(9)	20.85(6)
c (Å)	13.957(6)	26.796(19)	18.928(5)	19.202(8)	18.94(5)
α (deg)	71.288(17)	90	90	70.643(4)	90
β (deg)	79.596(19)	110.21(4)	99.878(5)	79.138(5)	99.19(9)
γ (deg)	83.765(11)	90	90	83.636(4)	90
V ($Å^3$)	1231.7(10)	4952(6)	3975.0(18)	1280.7(4)	4003(19)
T (K)	295(2)	295(2)	295(2)	295(2)	295(2)
Z	1	4	4	4	4
no. of independent reflns	3087 [R(int) = 0.0267]	3408 [R(int) = 0.0803]	3711 [R(int) = 0.0782]	2732 [R(int) = 0.0664]	4290 [R(int) = 0.0963]
no. of observed reflns [$I > 2\sigma(I)$]	1787	1942	2242	1751	2670
R1	0.0614	0.0843	0.0844	0.0683	0.0790
wR2[a]	0.1417	0.2329	0.2166	0.1606	0.1928

	6	**7a**	**7b**	**8**
chemical composition	$C_{50}H_{92}O_{12}Hf_2$	$C_{44}H_{76}ZrO_8$	$C_{44}H_{76}ZrO_8$	$C_{44}H_{76}HfO_8$
fw	1242.22	824.27	824.27	911.54
cryst syst	monoclinic	monoclinic	triclinic	monoclinic
space group	$P2(1)/n$	$P2/c$	$P\bar{1}$	$P2/c$
μ (mm^{-1})	3.464	0.273	0.279	2.211
a (Å)	10.714(4)	22.545(6)	12.086(7)	22.545(6)
b (Å)	20.285(8)	11.275(3)	19.33(4)	11.275(3)
c (Å)	14.321(6)	19.763(5)	21.135(8)	19.763(5)
α (deg)	90	90	97.71(10)	90
β (deg)	102.553(9)	106.550(7)	90.38(4)	106.550(7)
γ (deg)	90	90	105.79(18)	90
V ($Å^3$)	3038(2)	4816(2)	4703(10)	4816(2)
T (K)	295(2)	295(2)	293(2)	295(2)
Z	2	4	4	4
no. of independent reflns	3241 R(int) = 0.0536]	3275 [R(int) = 0.0493]	11321 [R(int) = 0.1489]	4447 [R(int) = 0.0729]
no. of observed reflns [$I > 2\sigma(I)$]	2243	2282	8393	2945
R1	0.0590	0.0826	0.0825	0.0763
wR2[b]	0.1300	0.2063	0.1546	0.1830

[a] $wR2(F^2) = [\sum w|F_o^2 - F_c^2|^2/\sum[F_o]^4)]^{1/2}$ and $w = 1/[\sigma^2(F_o^2) + (AP)^2 + (BP)]$, where $P = (F_o^2 + 2F_c^2)/3$; $A = 0.0903$, $B = 0$ for **1**; $A = 0.1693$, $B = 0$ for **2**; $A = 0.1448$, $B = 4.4412$ for **3**; $A = 0.0866$, $B = 0$ for **4**; and $A = 0.1308$, $B = 0$ for **5**. [b] $wR2(F^2) = [\sum w|F_o^2 - F_c^2|^2/\sum[F_o]^4)]^{1/2}$ and $w = 1/[\sigma^2(F_o^2) + (AP)^2+(BP)]$, where $P = (F_o^2+ 2F_c^2)/3$; $A = 0.0656$, $B = 12.9572$ for **6**; $A = 0.1187$, $B = 21.4816$ for **7a**; $A = 0$, $B = 28.6911$ for **7b**; and $A = 0.1127$, $B = 16.6151$ for **8**.

5, it was possible to localize the alternative positions for one such fragment. For the other fragments in structures **1**−**5**, this problem led to high anisotropy of the terminal carbon atoms and increased R factors. Another general problem of structures **1**−**5** is the rotational disorder of the alkyl groups of alkoxide ligands. This effect is especially pronounced in the structures of compounds **2** and **4**, where the differences in the sizes of ligands (both ^{n}Pr and ^{i}Pr in **2**) or slightly smaller size of the metal atom (Hf compared to Zr) result in an unresolved rotational disorder of these groups. All calculations were performed using the SHELXTL-NT program package[33] on an IBM PC. The figures are showing the thermal ellipsoids at the 10% probability level in order to see the connectivity avoiding the effects of thermal motion.

The structure of **7b** was determined at KTH Stockholm using a Kappa CCD diffractometer. This latter data collection was run at −120 °C. This example also shows that low-temperature experiments do not improve the quality of refinement hindered by the specific character of disorder in the structure.

Computation of Internal and Lattice Energies. To get more insight into the van der Waals interactions at work in $M(thd)_4$ compounds, we used the PACHA software[34] running on an IBM PC. The ability of this software to quantify the relative contributions of any kind of weak molecular interactions (hydrogen bonding, coordination links, $\pi-\pi$ stacking, van der Waals) responsible for the formation of a crystalline network has been demonstrated previously.[35,36] The method has its basis in a comparison of the internal energies (named EB hereafter) of a crystal to the internal energies of isolated building blocks extracted from the lattice, the observed difference being the lattice energy released when those building blocks come from infinity at their right place in the crystal. For structures **7a**, **7b**, and **8**, the raw data coming from X-ray diffraction has been used and the corresponding lattice energies should then be considered as being very rough approximations of true crystalline energies. For structure **7b**, it was noticed that methine protons on thd groups were absent from the X-ray data file. A new structure (named **7h**) has thus been generated by adding them in the O−C−C−C−O plane assuming bisection of the C−C−C bond angle and d(C−H) = 108 pm. For **7a** and **8**, it was not possible to add missing hydrogen atoms because of the strong disorder. From **8**, it was also possible to derive two structures

(33) *SHELXTL-NT Program Manual*: Bruker AXS: Madison, WI, 1998.

(34) Henry, M. *ChemPhysChem* **2002**, *3*, 561.

(35) Henry, M.; Hosseini, M. W. *New J. Chem.* **2004**, *28*, 897.

(36) Turner, D. R.; Henry, M.; Wilkinson, C.; McIntyre, G. J.; Mason, S. A.; Goeta, A. E.; Steed, J. W. *J. Am. Chem. Soc.* **2005**, *127*, 11063.

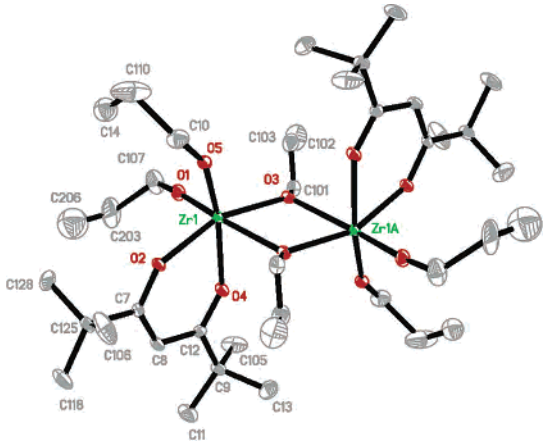

Figure 1. Molecular structure of $[Zr(O^nPr)_3(thd)]_2$ (**1**). Zr(1)−O(5) = 1.891(6) Å, Zr(1)−O(1) = 1.896(7) Å, Zr(1)−O(3) = 2.067(4) Å, Zr(1)−O(2) = 2.104(4) Å, Zr(1)−O(4) = 2.140(6) Å, Zr(1)−O(3)#1 = 2.158(5) Å, Zr(1)−Zr(1A) = 3.459(2) Å. The corresponding bond lengths for $[Hf(O^nPr)_3(thd)]_2$ (**4**) are as follows: Hf1−O5 = 1.891(17) Å, Hf1−O1 = 1.909(12) Å, Hf1−O3 = 2.043(19) Å, Hf1−O2 = 2.053(13) Å, Hf1−O4 = 2.165(12) Å, Hf1−O3 = 2.200(18) Å, Hf1−Hf1 = 3.4641(16) Å.

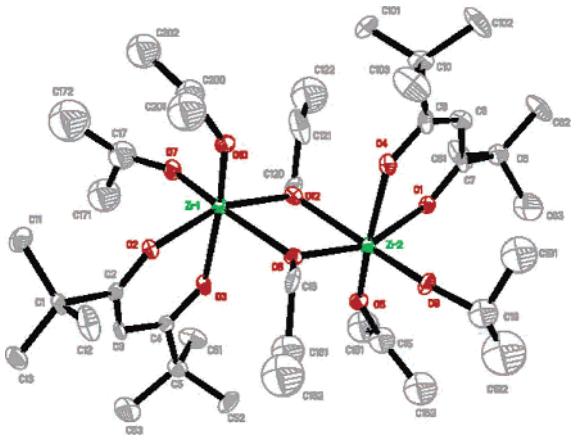

Figure 2. Molecular structure of $[Zr(O^iPr)_2(O^nPr)(thd)]_2$ (**2**). Selected bond lengths: Zr(1)−O(7) = 1.834(13) Å, Zr(1)−O(10) = 1.876(12) Å, Zr(1)−O(12) = 2.030(13) Å, Zr(1)−O(2) = 2.099(13) Å, Zr(1)−O(3) = 2.121(14) Å, Zr(1)−O(6) = 2.141(13) Å, Zr(1)−Zr(2) = 3.464(3) Å.

(named **8A** and **8B** hereafter) showing no disorder and differing only by the kind of isomer involved in building the 3D lattice. Corresponding internal and lattice energies have thus been estimated for these complexes without the further addition of missing H atoms.

Results and Discussion

The modification of zirconium *n*-propoxide and mixed-ligand precursors with 1 mol equiv of Hthd has provided **1** and **2**. The structures of these compounds (see Table 1, Tables 1 and 2 of the Supporting Information, and Figures 1 and 2) were determined by X-ray single-crystal studies as being $[Zr(O^nPr)_3(thd)]_2$ and $[Zr(O^iPr)_2(O^nPr)(thd)]_2$. These compounds display structures analogous to that obtained from zirconium isopropoxide with a corresponding amount of Hthd.[15] This latter compound was also obtained by us using the same technique as for **1** and **2** and avoiding the refluxing applied earlier by Fleeting et al.[15]

The largest difference between the monosubstituted complexes prepared in the present study and $[Zr(O^iPr)_3(thd)]_2$ is the presence of *n*-propoxide ligand in bridging positions. This less bulky ligand compared to isopropoxide causes a smaller metal−metal distance, i.e., 3.459(2) and 3.494(3) Å for **1** and **2** compared to 3.508(1) Å for $[Zr(O^iPr)_3(thd)]_2$. Also, the angle between the oxygens in bridging positions and metal atom decreases slightly, 70.1(2) and 69.4(5)° for **1** and **2** compared to 72.0(2)° for $[Zr(O^iPr)_3(thd)]_2$. Consequently, the metal−oxygen bond lengths for the bridging groups will also be shorter for **1** and **2**. The metal−oxygen bond lengths of the alkoxide ligands in terminal positions are shorter in complexes **1** and **2**, i.e., 1.891(6)−1.896(7) Å, 1.834(13)−1.876(12) Å and 1.931(2)−1.944(2) Å for **1**, **2**, and $[Zr(O^iPr)_3(thd)]_2$, respectively.

$$^1/_2[Zr(O^iPr)_4(^iPrOH)]_2 + Hthd \rightarrow {}^1/_2[Zr(O^iPr)_3(thd)]_2 + {}^iPrOH$$

$$^1/_4[Zr(O^nPr)_4]_4 + Hthd \rightarrow {}^1/_2[Zr(O^nPr)_3(thd)]_2\ (\mathbf{1}) + {}^nPrOH$$

$$^1/_2[Zr(O^nPr)(O^iPr)_3(^iPrOH)]_2 + Hthd \rightarrow {}^1/_2[Zr(O^nPr)(O^iPr)_2(thd)]_2\ (2) + {}^iPrOH$$

The synthesized compounds were further characterized by ^{1}H NMR. The spectrum obtained by us for $[Zr(O^iPr)_3(thd)]_2$ (depicted in Figure 3b) differs significantly from the one published by Fleeting et al.[15] In this latter work, two signals were observed in the region 5.6−6.0 ppm. In contrast, only one signal (at 5.81 ppm) is present in the spectra observed by us for $[Zr(O^iPr)_3(thd)]_2$ and **1** (Figure 3a). The signals at these chemical shifts are characteristic of the CH of the thd ligand; if the centrosymmetric structures of the compounds are preserved in solution, these ligands should be equivalent, producing only one such signal as has been observed in our work. The signal due to CH_3 of thd is present at 1.13 ppm and in both spectra with the expected ratio 1:18 to the CH signal in the integration.

Further interpretation of the spectra is complicated by the presence of residual solvent and parent alcohol, which are very difficult to remove completely by drying in a vacuum. The problem also lies in the fact that no heating can be applied on those systems on drying, as it leads to transformation of the compounds. The signals labeled with (*) in the spectra of $[Zr(O^iPr)_3(thd)]_2$ belong to toluene and hexane, whereas those at 1.55 and 4.05 ppm are assigned to 2-propanol. This implies that the remaining signal at 4.25 ppm is due to the CH of the propoxide ligands, suggesting that the alkoxide ligands in bridging and terminal groups are in fast interchange. The spectra obtained after storing the dried crystals for 2 months support this interpretation. During storage, the remaining solvents diffused through the septum; consequently, the spectrum mainly showed the expected signals for $[Zr(O^iPr)_3(thd)]_2$.

For compound **1**, the signals attributed to the alkoxide ligands in both terminal and bridging positions result in two signals in the NMR spectra. The signal at 3.93 ppm, attributed to the terminal CH_2 of the alkoxide ligands, has the required ratio 4:1 compared to the OCH signal of thd,

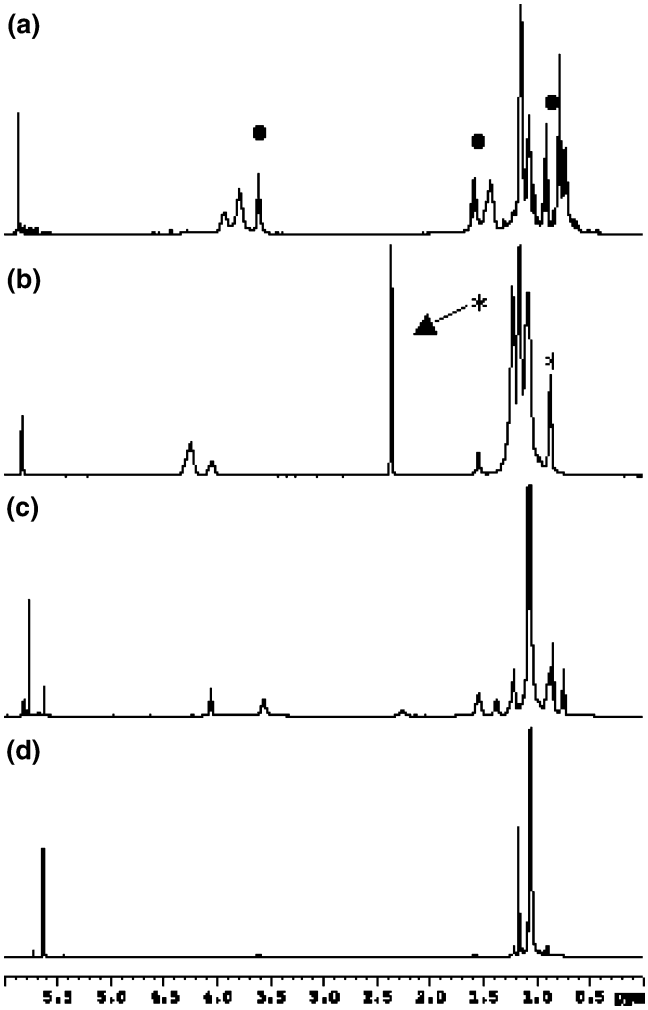

Figure 3. NMR spectra of (a) **1**, (b) $[Zr(O^iPr)_3(thd)]_2$, (c) **3**, and (d) $Zr(thd)_4$. The signals labeled with (*) belong to toluene and hexane and those labeled with (●) to *n*-propanol.

whereas the signal at 3.81 ppm is in a ratio 2:1 compared to the OCH signal of thd and is assigned to the alkoxide ligands in bridging position. The spectra display an unassigned signal at 3.60 ppm. This signal and the other signals marked with (●) match the positions and ratios of residual *n*-propanol.

The previously discussed compounds, i.e., $[Zr(O^iPr)_3(thd)]_2$ and **1**, have the same type of alkoxide ligands in both the bridging and terminal positions. Compound **2**, on the contrary, has *n*-propoxide ligands in bridging positions and isopropoxide ligands in terminal positions. This difference was clearly observed in the NMR spectra. The expected ratio of 3:4 (normalized on CH of the thd) for the terminal versus bridging positions was acquired.

The stability of modified precursors is a requirement for making them applicable for use in MOCVD. Both the solution and shelf, or solid-state, stability of **1**, **2**, and $[Zr(O^iPr)_3(thd)]_2$ have been examined. It was already mentioned above that $[Zr(O^iPr)_3(thd)]_2$, is relatively shelf stable. Upon storage for 2 months, the sample contained only a minor amount of a different phase. In the NMR spectra, an additional small signal could be seen in the region between 5.6 and 6.0 ppm. In contrast, the solution stability in $CDCl_3$ is rather limited; after 10 days, only ~40% of the signals in the region between 5.6 and 6.0 ppm was due to $[Zr(O^iPr)_3(thd)]_2$. The obtained spectrum was in appearance similar to that presented by Fleeting et al.[15] The second signal present in both groups' spectra, at a slightly lower chemical shift (~5.65 ppm) than that of CH of the thd in the initial complex, is most probably that of $Zr(thd)_4$. The refluxing during the synthesis of this compound already evidently leads to a mixture of several compounds. These data show clearly that the refluxing should be avoided in the modification of zirconium alkoxides, in contradiction to earlier recommendations by Mehrotra.[37]

$$[Zr(OR)_3(thd)]_2 \xrightarrow{\text{heat/time}} Zr(OR)_4 + Zr(thd)_4 + Zr(OR)(thd)_3$$

The stabilities of **1** and **2** were compared to that of $[Zr(O^iPr)_3(thd)]_2$. In $CDCl_3$, about 30% of **1** was still present after 10 days, and the spectra displayed 3 signals in the region between 5.6 and 6.0 ppm, whereas for **2**, only 20% of the total signals corresponded to the monosubstituted compound. In the latter sample, the formation of unmodified mixed-ligand precursor could clearly be observed. The presence of three signals suggests that, in addition to mono- and tetrasubstituted, there is at least one more type of species. The solution stability of **1** is thus on the same order of magnitude as that of $[Zr(O^iPr)_3(thd)]_2$, whereas that of **2** is significantly smaller. It should be noted that the data on the composition can be used only in a semiquantitative way. Effects due to concentration differences and different dryness of the compounds, e.g., parent alcohol can enhance transformation processes,[38] are not taken in account in this study. For each sample, approximately the same amount of compound was dissolved and the compounds were dried as well as possible; however, the presence of residue alcohol in the samples can be seen in the NMR spectra in Figure 3.

The solid state stability was significantly lower for **1** and **2** compared to that of the isopropoxide complex. After two months, the signal at 5.87 ppm was only ~10% of the total in that region for **1** and even less for **2**. The transformation again involved the formation of two other compounds for **1** and even three different species for **2**, i.e., there were 4 signals between 5.6 and 6.0 ppm. The lack of solid-state stability for **1** and **2** provides a plausible explanation for the slightly deviating values obtained by the element analysis.

On basis of the their solid-state stability, it can be seen that **1** and **2** are more like each other than like $[Zr(O^iPr)_3(thd)]_2$. A similar trend can be seen in the mass spectrometry data (Table 2). Compounds **1** and **2** show clear dimeric behavior in the gas phase, the major component in the gas-phase being $Zr(OPr)(thd)_2$ $m/z = 515$ (100%). For $[Zr(O^iPr)_3(thd)]_2$, the major fraction in the gas phase is found at $m/z = 391$(100%) corresponding to the monomeric $Zr(O^iPr)_2(thd)^+$.

(37) Pathak, M.; Bohra, R.; Mehrotra, R. C.; Lorenz, I. P.; Piotrowski, H. *Z. Anorg. Allg. Chem.* **2003**, *629*, 2493.
(38) Kessler, V. G. Chemistry and Solution Stability of Alkoxide Precursors. In *Handbook of Sol−Gel Science and Technology*; Kozuka, H., Ed.; Kluwer Academic Publishers: Boston, 2004; Chapter 1.

Table 2. Interpretation of *m*/*z*(I) Spectrum of **1**, **2**, $[Zr(O^iPr)_3(thd)]_2$, $[Hf(O^iPr)_3(thd)]_2$, **3**, and **4**

	1	**2**	$[Zr(O^iPr)_3(thd)]_2$	$[Hf(O^iPr)_3(thd)]_2$	**3**	**4**
M(thd)(OH)					290 (16)	379 (11)
$M(thd)(OH)_2$			307 (75)			396 (34)
$Zr(OPr)_2(thd-C_3H_8)$			347 (27)			
$M(OPr)_2(thd)$	391 (28)	391 (37)	391 (100)	479 (28)		479 (42)
$M(thd)_2$	459 (73)	459 (81)	459 (100)	549 (25)	459 (14)	
$Zr(OPr)(thd)_2$	515 (100)	515 (100)	515 (100)	604 (100)	515 (100)	604 (100)
$M(thd)_2(thd-C_3H_8)$		583 (25)		673 (56)	583 (69)	
$Zr_2(OPr)_2(thd)(thd-C_3H_8)$			615 (10)			
$M(thd)_3$		639 (21)		729 (30)	639 (75)	
$Zr_2(OPr)_6(thd)$			717 (9)			
$Zr_3(OPr)_8$	739 (6)	739 (21)				
$M_2(OPr)_4(thd)_2$	785 (16)	785 (14)	785 (13)	965 (29)		
$Zr_2(OPr)_5(thd)_2$	845 (11)	843 (8)	843 (5)			

Despite the stability, especially in the solid state, and the gas-phase behavior of $[Zr(O^iPr)_3(thd)]_2$, it has resulted in only a few publications dealing with the preparation of materials.[16−18] What might have had influence on the applicability of $[Zr(O^iPr)_3(thd)]_2$ is that its synthesis involved refluxing, which certainly led to the disproportionation with formation of complexes containing more thd ligands. The formation of another compound, supposedly $Zr(thd)_4$, can clearly be seen from the NMR spectra presented by Fleeting et al.[15] The presented monosubstituted compounds **1** and **2**, containing *n*-propoxide ligands in the bridging position, are significantly less stable in both solid state and solution. Another difference with $[Zr(O^iPr)_3(thd)]_2$ is that **1** and **2** tend to remain dimeric in the gas phase where $[Zr(O^iPr)_3thd)]_2$ is predominantly monomeric. It can thus be concluded that the physicochemical (i.e., solution and gas-phase stability) properties of **1** and **2** make them not suitable for application in CVD or liquid delivery MOCVD.

The presence of three or more signals in the NMR spectra of aged **1** and **2** indicated the presence of more multiple-thd-substituted compounds. According to previous studies,[15,23] this should be a disubstituted species. To investigate the structure of this higher-substituted compound, we modified $[Zr(O^iPr)_4(^iPrOH)]_2$ and $[Zr(O^nPr)(O^iPr)_3(^iPrOH)]_2$ with 2 mol equiv of Hthd. In both samples, crystals formed upon storage at −30 °C. The ones obtained from the sample with zirconium isoproxide were identified as being $[Zr(O^iPr)_3(thd)]_2$, whereas, somewhat surprisingly, a trisubstituted $Zr(O^iPr)(thd)_3$ (**3**, Table 1, Table 3 of the Supporting Information, and Figure 4) compound was obtained from the mixed-ligand precursor. The structure of this mononuclear compound will be discussed in more detail below.

$$^1/_2[Zr(O^iPr)_4(^iPrOH)]_2 + 2Hthd \rightarrow {}^1/_4[Zr(O^iPr)_3(thd)]_2 + {}^1/_2Zr(O^iPr)(thd)_3\ (\mathbf{3}) + 2^iPrOH$$

$$^1/_2[Zr(O^nPr)(O^iPr)_3(^iPrOH)]_2 + 2Hthd \rightarrow {}^1/_4[Zr(O^nPr)(O^iPr)_2(thd)]_2\ (\mathbf{2}) + {}^1/_2Zr(O^iPr)(thd)_3\ (\mathbf{3}) + 2^iPrOH$$

$$^1/_4[Zr(O^nPr)_4]_4 + 2Hthd \rightarrow \cdots \rightarrow {}^1/_8[Zr(O^nPr)_4]_4 + {}^1/_2Zr(thd)_4\ (\mathbf{7}) + 2^nPrOH$$

We also attempted to obtain and isolate this mononuclear compound from zirconium isopropoxide. Compound **3** could successfully be isolated from a synthesis with zirconium isopropoxide after the removal of $[Zr(O^iPr)_3(thd)]_2$ through crystallization, as described in the Experimental Section. The synthesis that was presented for the preparation of $Zr(O^iPr)_2(thd)_2$, i.e., interaction of the zirconium isopropoxide with 2 mol equiv of Hthd and refluxing, was also carried out. The obtained crystals were again identified as $[Zr(O^iPr)_3(thd)]_2$. It is likely, on the basis of the amount of added modifier, that for both precursors, $[Zr(O^iPr)_4(^iPrOH)]_2$ and $[Zr(O^nPr)(O^iPr)_3(^iPrOH)]_2$, a mixture of mono- and trisubstituted compounds is formed upon modification. Upon cooling, the compound that crystallizes easiest will be formed initially. In the case of zirconium isopropoxide, the crystals of the monosubstituted compound are formed first, whereas for the sample prepared from the mixed-ligand alkoxide, it is **3** that crystallizes easiest.

The trisubstituted compounds obtained from the two different zirconium alkoxides were characterized by NMR. A spectrum obtained from the system with zirconium isopropoxide as the precursor is depicted in Figure 3c. Depending on the sample, there are three or four signals

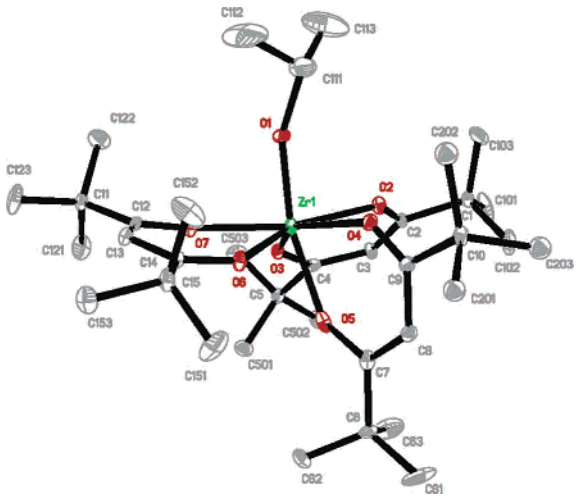

Figure 4. Molecular structure of $Zr(O^iPr)(thd)_3$ (**3**). Selected bond lengths of 3: Zr(1)−O(1) = 1.847(8) Å, Zr(1)−O(5) = 2.017(10) Å, Zr(1)−O(7) = 2.091(8) Å, Zr(1)−O(3) = 2.108(7) Å, Zr(1)−O(2) = 2.123(8) Å, Zr(1)−O(6) = 2.165(8) Å, Zr(1)−O(4) = 2.185(8) Å. The corresponding bond lengths of the hafnium isomorph $Hf(O^iPr)(thd)_3$ (**5**) are as follows: Hf(1)−O(1) = 1.810(12) Å, Hf(1)−O(5) = 2.050(13) Å, Hf(1)−O(3) = 2.116(12) Å, Hf(1)−O(7) = 2.123(12) Å, Hf(1)−O(6) = 2.154(12) Å, Hf(1)−O(2) = 2.165(12) Å, Hf(1)−O(4) = 2.161(14) Å.

present in the region between 5 and 6 ppm. The major signal at 5.80 ppm is assigned to **3**, and the other signals due to this compound were identified at 1.02 and 1.07 ppm, corresponding to CH_3 of the propoxide and thd, respectively, and at 4.36 ppm, corresponding to the CH of the alkoxide ligand. The two minor signals in all spectra are assigned to $[Zr(O^iPr)_3(thd)]_2$ (5.81 ppm) and $Zr(thd)_4$ (5.62 ppm); in some spectra, a signal was observed at 5.67 ppm, which is most likely due to a hydroxodi-thd-substituted compound. There are no indications for the existence of a disubstituted compound "$Zr(O^iPr)_2(thd)_2$". The full interpretation of the signals of the various compounds is provided in the Experimental Section.

The NMR spectra obtained for **3** prepared from the mixed-ligand precursor display at least five minor signals present in the region between 5.5 and 6.0 ppm. The presence of these five signals is not unexpected, because the unmodified precursor has both isopropoxide and *n*-propoxide ligands, thereby allowing the formation of **1** and **2** during its decomposition in time and the ability to form a compound analogous to **3** with an *n*-propoxide ligand. The complexity of the spectra prevented further quantitative interpretation.

The *n*-propoxide analogue of compound **3** was synthesized from zirconium *n*-propoxide modified with 3 mol equiv of Hthd, as described in the Experimental Section. However, the obtained crystals were not of X-ray quality. Single crystals that were identified as $Zr(O^nPr)(thd)_3$ were obtained as a side product in the synthesis (see ref 30 for more details) with zirconium *n*-propoxide, strontium *n*-propoxide, and 2 mol equiv of Hthd in a mixture of *n*-propanol and toluene. The full refinement of the XRD structure was not accomplished because of a rather complex unresolved disorder in the *n*-propel radical, yet the existence of trisubstituted zirconium *n*-propoxide was clearly demonstrated. The metal−oxygen bond of the alkoxide ligands is longer in $Zr(O^nPr)(thd)_3$ compared to that in **3**, 1.847(8) and 1.924(11) Å, respectively. The increase in the bond length of $Zr(O^nPr)(thd)_3$ is in good agreement with the decreased inductive effect of *n*-propoxide compared to that of isopropoxide ligands.

The solution and solid-state stability of these compounds was also investigated. Two phenomena should be taken into account. The stability of **3** obtained from zirconium isopropoxide was investigated in both solid state and solution. In both situations, it could clearly be seen that the compound was not stable in time, but after two months in the solid state and two weeks in solution, there was still a fair amount of **3** present. However, it was not possible to quantify the stability because of the occurrence of two phenomena. The position of different signals is strongly dependent on the temperature; in order to distinguish the different species, we performed the experiments at low temperature, i.e., 243 K. However, the solubility of $Zr(thd)_4$ is very low (the reasons as to why that is will be discussed below) and it cannot be excluded that at the low temperature of the experiment, the crystallization of $Zr(thd)_4$ occurs. It could be seen from the obtained complex NMR spectra that the stability is significantly less if **3** is prepared from the mixed-ligand precursor. The faster transformation toward $Z(thd)_4$ is probably due to the facilitating effect of the residual alcohol.[38]

Mass spectrometry experiments were performed on **3** obtained from zirconium isopropoxide. The main compounds in the gas phase, as can be seen in Table 2, were found at 515 (100%), 583 (69%) and 639 (75%) *m*/*z*. They are assigned to $Zr(O^iPr)(thd)_2$, $Zr(thd)_2((CMe_3C)COCHC(H)O)$, and $Zr(thd)_3$, respectively. The fragments in the gas phase are mainly trisubstituted, as can be expected for **3**. Similar mass spectrometry results were published by Jones et al.,[17] but the authors assigned the fragments to origins from "$Zr(O^iPr)_2(thd)_2$".

An NMR spectrum was taken of the purchased commercial product that was claimed to be "$Zr(O^iPr)_2(thd)_2$". In the obtained spectrum, the ratio between thd and alkoxide ligands is 3:1 on the basis of the signals in the regions between 5.5 and 6.0 ppm and 3.5−4.5 ppm. There is one major signal present around 5.62 ppm that corresponds to the position of $Zr(thd)_4$, and a minor one (∼10% of the major signal) at 5.80 ppm that indicates the presence of **3**. This composition suggests the presence of the unmodified precursor and that the solid modified product contains only ∼2.5% of alkoxide ligands (when it should contain 50%).

It can be concluded that the modification of zirconium propoxide precursors with more than 1 mol equiv of Hthd involves the formation of a trisubstituted compound. This is in contrast to the generally assumed formation of a disubstituted compound. The isolation of purely trisubstituted compound is complicated, because the mono- and tetrasubstituted compounds tend to crystallize easier in most cases, resulting in the obtaining of these compounds or a mixture of these compounds. The trisubstituted compounds have the tendency to rearrange into the thermodynamically stable $Zr(thd)_4$, and residual alcohol enhances this transformation.

Having an understanding of the chemistry involved in the Hthd modification of zirconium propoxide precursors, it was interesting to examine if hafnium isopropoxide is modified in an analogous manner. The structure of the monosubstituted intermediate, $[Hf(O^iPr)_3(thd)]_2$, was published by Fleeting et al.[15] The stability of this compound was evaluated by NMR, and it was seen that its behavior upon aging in the solid state and solution was analogous to that of $[Zr(O^iPr)_3(thd)]_2$. In solid state, the compound is fairly stable, whereas in solution, rearrangement to $Hf(thd)_4$ occurs.

The modification of hafnium *n*-propoxide with 1 mol equiv of Hthd resulted in the formation of $[Hf(O^nPr)_3(thd)]_2$ (**4**, Table 1, and Table 4 of the Supporting Information), which is, to the best of our knowledge, the first structural determination of a hafnium *n*-propoxide derivative. The compound is isomorphous with **1**, for which the molecular structure is depicted in Figure 1. The presence of *n*-propoxide ligands causes the metal−metal distance in the structure to be smaller in **4** compared to that of $[Hf(O^iPr)_3(thd)]_2$, i.e., 3.4641(16) and 3.476 Å, respectively. This trend was also observed in the analogous zirconium compounds; however, the difference is not as significant as was observed for zirconium. The metal−oxygen bond length of the alkoxide ligands in **4** are

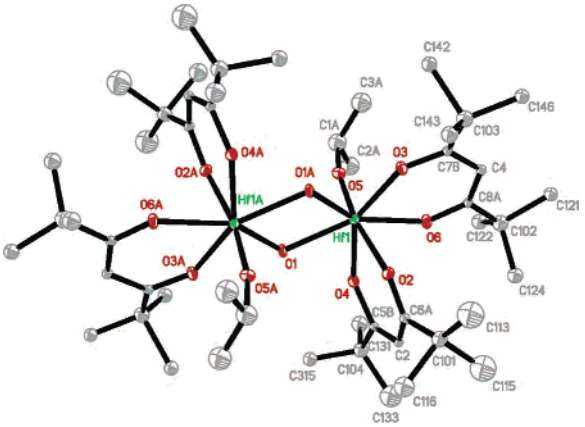

Figure 5. Molecular structure of $[Hf(O^iPr)(thd)_2(OH)]_2$ (**6**). Selected bond lengths: Hf(1)−O(5) = 1.886(10) Å, Hf(1)−O(1)#1 = 2.105(8) Å, Hf(1)−O(2) = 2.112(9) Å, Hf(1)−O(1) = 2.129(8) Å, Hf(1)−O(3) = 2.141(9) Å, Hf(1)−O(4) = 2.145(9) Å, Hf(1)−O(6) = 2.193(8) Å, Hf(1)−Hf(1)#1 = 3.5621(15) Å.

shorter than those in $[Hf(O^iPr)_3(thd)]_2$, i.e., 1.891(17) and 1.909(12) Å for **4** and 1.927 and 1.953 Å for $[Hf(O^iPr)_3(thd)]_2$. The observed decrease in metal−oxygen bond length is in agreement with the observation, discussed above, for zirconium. The solution stability of this compound is rather poor; after 55 h in solution ($CDCl_3$), 30% of **4** had already disappeared.

More interesting is the modification behavior of hafnium isopropoxide with more than 1 mol equiv of Hthd. A sample of the precursor with 2.5 mol equiv of Hthd was prepared. The first crystals obtained were identified as being $[Hf(O^iPr)_3(thd)]_2$; after removal of these initial crystals, two other types of crystals were obtained. The first type was identified as $Hf(O^iPr)(thd)_3$ (**5**, Table 1, and Table 5 in the Supporting Information), and this compound is analogous to **3**.

Structures **3** and **5** contain one alkoxide and three thd ligands. The metal−oxygen bond length of the alkoxide ligand is slightly shorter in **5**, i.e., 1.810(12) and 1.847(8) Å for **5** and **3**, respectively. However, the metal−oxygen bond length of the thd oxygen opposite the alkoxide ligand is slightly longer in **4**, i.e., 2.050(13) and 2.017(10) Å for **5** and **3**, respectively. The other metal−oxygen bond lengths in **5** are between 2.116(12) and 2.165(12) Å, whereas the difference in lengths in **3** is significantly larger, at 2.091(8)−2.185(8) Å.

The other needle-shaped crystals that were obtained upon the modification of hafnium isopropoxide with 2.5 mol equiv of Hthd were identified as being $[Hf(O^iPr)(thd)_2(OH)]_2$ (**6**, Table 1, Figure 5, and Table 6 in the Supporting Information).

Compound **6** is a microhydrolysis product. The required water for this reaction is probably provided upon transferring the solution, which was decanted from the first crystals to a new flask. The compound **6** can be quantitatively formed from **5** and $[Hf(O^iPr)_3(thd)]_2$ upon introduction of a stoichiometric amount of water, as described in the Experimental Section. The NMR study of the freshly dried reaction mixture does not show any signals other than those corresponding to **5** and $[Hf(O^iPr)_3(thd)]_2$.

$$^1/_2[Hf(O^iPr)_4(^iPrOH)]_2 + 2Hthd \rightarrow {}^1/_4[Hf(O^iPr)_3(thd)]_2 + {}^1/_2Hf(O^iPr)(thd)_3\ (\mathbf{5}) + 2\,^iPrOH$$

$$^1/_4[Hf(O^iPr)_3(thd)]_2 + {}^1/_2Hf(O^iPr)(thd)_3 + H_2O \rightarrow {}^1/_2[Hf(OH)(O^iPr)(thd)_2]_2\ (\mathbf{6})$$

The difference between **6** and $[Hf(O^iPr)_3(thd)]_2$[15] is the OH group in the bridging position, which allows for the formation of a complex with one more alkoxide ligand replaced by a thd ligand. The less bulky ligand in the bridging position leads to a decrease in the O(1)−Hf(1)−O(1A) angle in **6** compared to this angle in $[Hf(O^iPr)_3(thd)]_2$, 65.4(4) and 72.0(2)°, respectively. The metal−oxygen bond lengths of the bridging ligands are on the same order (2.129(8) and 2.105(8) Å for **5** and 2.192(5) and 2.102(5) Å for $[Hf(O^iPr)_3(thd)]_2$), resulting in slight increase in the metal−metal distance (3.5621(15) vs 3.476(1) Å). The metal−oxygen bond length of the alkoxide ligand is slightly shorter in **6** than for those in $[Hf(O^iPr)_3(thd)]_2$ (1.886(10) Å versus 1.927(6)−1.953(6) Å). The presence of a hydroxide group in the structure of this compound is well-reflected by its IR spectrum (a sharp band at 3690 cm^{-1} together with a number of weak bands at 3440, 3356, and 3178 cm^{-1}, reflecting the presence of a system of intramolecular hydrogen bonds, e.g., O(1)−H(1)···O(4) = 2.517(8) Å). Even the ^1H NMR spectrum has a clear resolution of methyl group signals that can be interpreted as being an indication of less steric tension for one ^{t}Bu group in the two thd ligands. After the isolation of **6**, there was an attempt to see whether an analogous zirconium compound existed. We were not able to isolate such a complex, and its formation could not be unequivocally traced in the NMR spectra. This observation is in good agreement with the generally observed trend of higher stability for dimeric aggregates derived from 5d transition-metal atoms compared to 4d ones.[38]

It can be concluded that the modification of hafnium isopropoxide with Hthd proceeds in the same manner as for zirconium isopropoxide. For both precursors, mono- and trisubstituted intermediates are formed, whereas a stable microhydrolyzed compound **6** could be isolated only for hafnium.

The main interest in the structural characterization of the tetra-thd-substituted complexes of zirconium and hafnium was to reveal the reasons for their unusual physicochemical properties. $M(thd)_4$, M = Zr, Hf, are known to be very poorly soluble in the hydrocarbon solvents and have relatively poor volatility in comparison to other mononuclear thd derivatives of transition metals. The slightly higher solubility in aromatic hydrocarbons can be attributed to a higher solvation ability of these solvents compared to the aliphatic ones. We succeeded in the preparation of X-ray quality single crystals of $Zr(thd)_4$ (**7a** and **7b**, i.e., two different polymorphs were obtained; Table 1, Tables 7a and 7b in the Supporting Information, and Figure 6) and $Hf(thd)_4$ (**8**; Table 1, Table 8 in the Supporting Information, and Figure 6). The ^1H NMR spectra of these compounds were as expected for these compounds. The mass spectra of $M(thd)_4$ are also in good agreement with their molecular structures and contain the

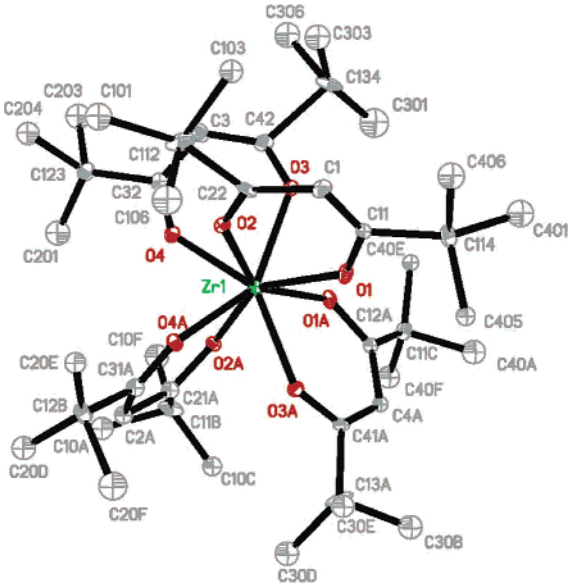

Figure 6. Molecular structure of $Zr(thd)_4$ (**7a** and **7b**). Selected bond lengths of **7a**: Zr(1)−O(4) = 2.127(8) Å, Zr(1)−O(1) = 2.130(7) Å, Zr(1)−O(2) = 2.151(9) Å, Zr(1)−O(3) = 2.197(9) Å. Selected bond lenghts for **8**: Hf(1)−O(4) = 2.109(10) Å, Hf(1)−O(1) = 2.115(10) Å, Hf(1)−O(2) = 2.174(10) Å, Hf(1)−O(3) = 2.183(11) Å.

Table 3. Interpretation of *M*−*Z* (I) Spectrum of **7** and **8**

	7	**8**
Zr((MeC)COCHC(H)O)(OCCHCO)	291 (14)	
[Hf(thd)−C_2H_4]		336 (12)
Zr((MeC)COCHC(CMe_3)O)(OCCHCO)	393 (18)	393 (8)
$Zr(thd)_3$	639 (100)	639 (12)
$Hf(thd)_3$		729 (100)

$M(thd)_3^+$ ions as the most intensive fragments (see Table 3), which corresponds to the dissociation of one ligand commonly observed through the electron impact. It should be noted, with respect to the observation of zirconium compounds in the MS spectra of **8**, that hafnium samples always contain up to 2% zirconium. The gas-phase content of the latter can be higher because of the relatively higher volatility of its compounds. The molecular structures of compounds **7a**, **7b**, and **8** are identical: eight oxygen atoms, forming an Archimedes antiprism, surround the metal atoms. The coordination of each thd ligand is slightly asymmetric, with one shorter M−O distance of about 2.13 Å and one longer distance of about 2.15−2.20 Å. The molecules in total have spheroid topology (Figure 6).

Figure 7 shows that the structure of **7b** consists of a stacking of almost-hexagonal 2D layers. Similar hexagonal layers are found in the structure of **7a**. The projections shown in Figure 8 make it apparent that in both structures, the molecules in adjacent layers are not positioned behind each other (implying closer packing) but are not perfectly close-packed. The difference between the polymorphs **7a** and **7b** can be understood by comparing the equivalent projections of the two structures (the view along the *b* axis for **7a** is equivalent to the view along the *a* axis for **7b**, see Figure 8). The crystal structure of **7a** can be considered as being a more-symmetric ABAB... close packing of spheroids, whereas that of **7b** can be idealized as being a slightly less symmetric ABCABC... packing. Not quite surprisingly, the triclinic

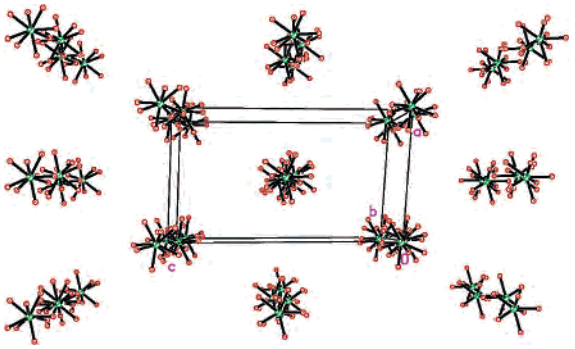

Figure 7. Almost-hexagonal close packing of $Zr(thd)_4$ viewed along the *c* axis. For clarity, the C and H atoms are not displayed.

structure formed from more-dilute solutions stays even for denser packing, with a unit cell volume of 4703(10) $Å^3$ compared to 4816(2) $Å^3$ for the monoclinic cell. Calculation of the distances between nearest methyl carbon atoms of the neighboring molecules gives an average of 4.4 Å, which is a relatively short distance indicating strong van der Waals interactions. The latter are supposedly responsible in combination with the dense packing effect for the low solubility and volatility of these compounds. The packing of the spheroids in **7a**, **7b**, and **8** requires a bigger and less symmetric unit cell compared to other known tetrakis derivatives of zirconium and hafnium such as $Zr(acac)_4$ [39] (*C*2/*c*) or $Hf(^tBuCOCHCO^iPr)_4$ [40] (*C*2/*c*), where the more-regular and less-symmetric nature of ligands permits a packing in a more-organized and less-uniform manner.

To be more quantitative, the internal energy of **7b** has been evaluated as being EB(**6b**) = −24 061 kJ mol^{-1}, corresponding to 4 complexes per unit cell. This has to be compared with the internal energy EB of the two crystallographically nonequivalent complexes characterized by EB(Zr1) = −5991 kJ mol^{-1} and EB(Zr81) = −6042 kJ mol^{-1}. The lattice energy is then E_{net}(**7b**) = 2[EB(Zr1) + EB(Zr81)] − EB(**7b**) = +5 kJ mol^{-1}. This almost-zero value is well in line with the high steric hindrance occurring in such complexes and would even mean that almost nothing is gained by packing them in a 3D network. As methine protons on thd groups were missing in this structure, the effect of adding them was investigated; this led to EB(**7h**) = −24 073 kJ mol^{-1}, EB(Zr1) = −5994 kJ mol^{-1}, and EB(Zr81) = −6045 kJ mol^{-1}. As can be easily checked, this does not change the lattice energy, which remains slightly positive. Knowing that the enthalpy of association in the crystal should be endothermic, it follows that the crystal formation should be entirely driven by entropy effects. In other words, there is no doubt that in solution, a large number of solvent molecules should be immobilized around these complexes, leading to a large and positive Δ*S* after crystallization. For the same reasons, it follows that solubility should be rather low, because of the large change in solvent structure that is needed for putting complexes in solution. To see if such considerations also apply to **7a**, we have investigated

(39) Clegg, W. *Acta Crystallogr., Sect. C* **1987**, *43*, 789.
(40) Pasko, S. V.; Hubert-Pfalzgraf, L. G.; Abrutis, A.; Richard, P.; Bartasyte, A.; Kazlauskiene, V. *J. Mater. Chem.* **2004**, *14*, 1245.

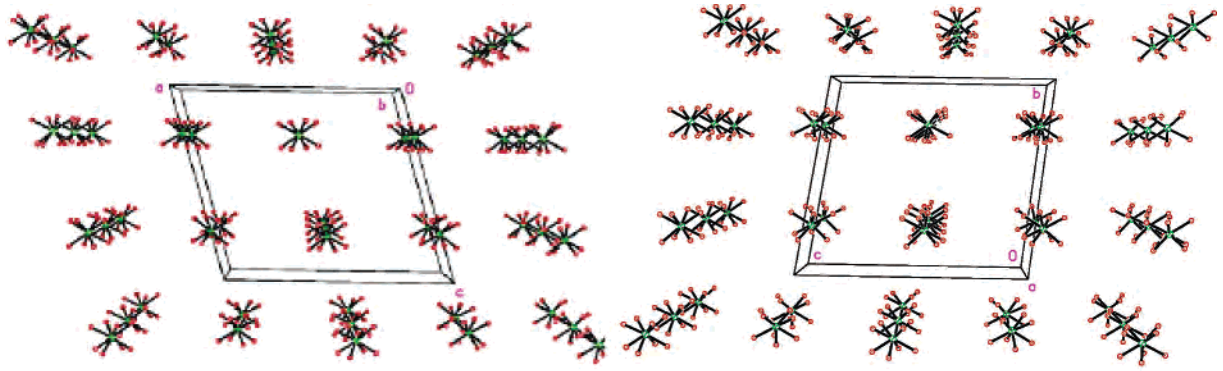

Figure 8. Comparison of the equivalent projections of **7a** and **7b**; **7a** viewed along the *b* axis is equivalent to the view along the *a* axis for **7b**. For clarity, the C and H atoms are not displayed.

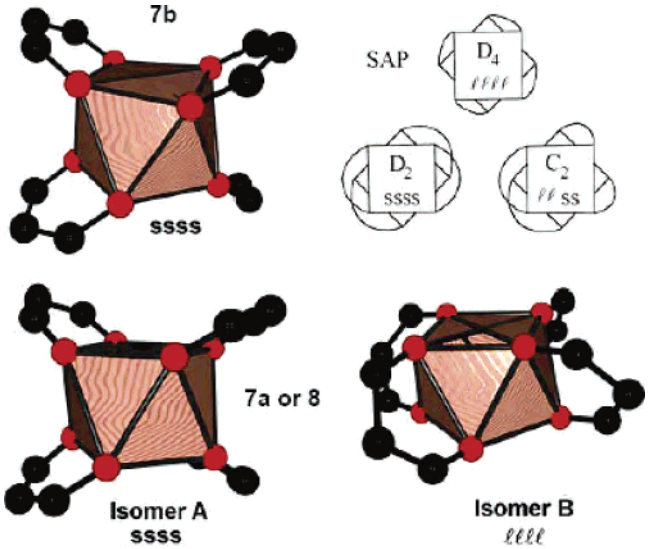

Figure 9. Structural and topologic description of the isomers in the structure **7b**.

this compound; this led to EB(**7a**) = −23792 kJ mol^{-1}, EB(Zr1) = −5950 kJ mol^{-1}, and EB(Zr2) = −5944 kJ mol^{-1}. The corresponding lattice energy is then found to be slightly negative E_{net}(**7a**) = −4 kJ mol^{-1}. This very small value demonstrates again that, as in the case of **7b**, crystallization and solubility are also entropy-controlled. Quite similar conclusions apply for **8**, despite higher internal energies: EB(**8**) = −20 042 kJ mol^{-1}, EB(Hf1) = −4988 kJ mol^{-1}, and EB(Hf2) = −5032 kJ mol^{-1}, which leads to E_{net}(**8**) = −2 kJ mol^{-1}.

It is also worth noting that in the case of the Zr(thd)$_4$, the observed kinetic effect (quick formation of **7a** followed by slow recrystallization of **7b**) is due to the existence of two different isomers crystallizing within the same network (Figure 9). **7a** or **8** should then be viewed as a random mixture of two isomers displaying D_2 and D_4 point group symmetry. From the observation that **7b** is the thermodynamic end product, it follows that the D_4 isomer should be less-solvated in solution than the D_2 isomer. To see if some enthalpy effect should be associated with the intergrowth of two networks based on isomers displaying D_2 and D_4 symmetry, respectively, we have generated two crystalline models derived from the available X-ray data of **8**. For **8A**, a net based on the stacking of D_2 isomers, we found EB(**8A**) = −19 584 kJ mol^{-1}, EB(Hf1) = −4934 kJ mol^{-1}, and EB(Hf2) = −4857 kJ mol^{-1}, leading to E_{net}(**8A**) = −2 kJ mol^{-1}, whereas for **8B**, a net based on the stacking of D_4 isomers, we found EB(**8B**) = −19 708 kJ mol^{-1}, EB(Hf1) = −4872 kJ mol^{-1}, and EB(Zr2) = −4982 kJ mol^{-1}, which leads to E_{net}(**8B**) = 0 kJ mol^{-1}. It follows that enthalpy effects associated with the mixing of both isomers should be quite low and that crystallization should be driven by entropy effects.

Conclusions

The modification of zirconium and hafnium propoxide precursors with Hthd involves mono- and trisubstituted intermediate compounds. The modification does not involve a bis-substituted compound, and thus, the commercial product that is claimed to be "Zr(O^{i}Pr)$_2$(thd)$_2$" most commonly used for the MOCVD preparation of ZrO_2 does not exist. No evidence was found for the presence of such a compound in either zirconium or hafnium-based systems. Formation of the dimeric hydroxo-di-thd-substituted complex could be proved only for hafnium-based system and occurs on microhydrolysis.

All heteroleptic intermediates are eventually transformed to the thermodynamically stable Zr(thd)$_4$ or Hf(thd)$_4$. The compounds obtained from isopropoxide precursors showed a higher stability than those with *n*-propoxide ligands or a combination of both types. In addition, it is important to note that residual alcohol facilitates the transformation and strongly enhances its rate.

The unusually low solubility and volatility of M^{IV}(thd)$_4$ has been shown to be due to close packing and strong van der Waals interactions in the crystal structures of these compounds.

Acknowledgment. The authors are very grateful to Rolf Andersson for the assistance with the NMR analysis and to Suresh Gohil for performing the mass spectrometry experiments. G.I.S. is grateful to The Netherlands Organization for Scientific Research (NWO) and EXXONMOBIL Chemical Benelux for facilitating his research at SLU with a travel grant and travel award, respectively. This work has been carried out at the Department of Chemistry, SLU, in the framework of the project "molecular precursors and molecular models of nanoporous materials".

Supporting Information Available: FT−IR spectra of the compounds (pdf); crystallographic data for the structural analysis (cif). This material is available free of charge via the Internet at http://pubs.acs.org. The crystallographic data have also been deposited with the Cambridge Crystallographic Data Centre. Copies of this information can be obtained free of charge via www.ccdc.cam.ac.uk/conts/retrieving.html (or from the Cambridge Crystallographic Data Centre, 12, Union Road, Cambridge CB2 1EZ, UK; fax: +44-1223-336033; e-mail: deposit@ccdc.cam.ac.uk).

IC051674J